

Supplementary Materials: Scheduling of Maintenance Tasks and Routing of a Joint Vessel Fleet for Multiple Offshore Wind Farms

Nora Tangen Raknes, Katrine Ødeskaug, Magnus Stålhane and Lars Magnus Hvattum

1. Small Numerical Example

To illustrate the mathematical model presented in the paper, a simple numerical example with two wind farms and a planning period of two shifts is presented. There are 30 turbines in each wind farm and a total of seven maintenance tasks generated for the planning period. The vessel fleet consists of two vessels, one AV and one SES. The AV is located at the depot at the beginning of the planning period, hence, it can stay offshore for the entire planning period if it departs from the depot. The weather windows for both the AV and the SES are entirely open during both shifts, and for both shifts it is desirable to perform extra preventive maintenance due to low energy production. The input data of the example are summarized in Tables S1–S3.

Table S1. Input data of the numerical example of the mathematical model.

	Number
Wind farms	2
Corrective tasks	5
Desired preventive tasks	1
Generated preventive tasks	2
AVs	1
SESeS	1
Regular CTVs	0
Shifts	2
Hours in a shift	12

Table S2. Generated tasks and corresponding task input data of the numerical example of the mathematical model.

Wind farm	Task	Task Type	Duration of Task (h)	Required Technicians	Vessel Type Compliance
1	1	Manual Reset	3	2	All
1	2	Manual Reset	3	2	All
1	3	Alarm	0.5	2	All
1	4	Alarm	0.5	2	All
1	5	Alarm	0.5	2	All
1	6	Preventive	60	3	All
2	7	Preventive	60	3	All

Table S3. Input data on vessels of the numerical example of the mathematical model.

	Number of Vessels	Travel Time to Wind Farm 1 (h)	Travel Time to Wind Farm 2 (h)	Travel Time between Farms (h)	Internal Wind Farm Transportation Time (h)	Transfer Time (h)
AV	1	3.60	3.15	2.25	0.19	0.5
SES	1	0.93	0.81	-	0.05	0.5

An illustration of the routing and the tasks performed during the two shifts are given in Figures S2 and S3. The turbines of the two wind farms are illustrated by circles and the turbines that require maintenance are numbered with maintenance task numbers. The routes of the vessels are represented by arcs. How Figure S2 and S3 show the order that the turbines are visited in, the number of technicians onboard the vessels after each turbine visit, and the time period of the shift when the turbines are shut down, are explained by Figure S1. The turbines are shut down from the moment a vessel arrives at the turbine until the vessel has departed the turbine after picking up the technicians. This includes the time of transferring technicians to the turbine, performing the task, potential waiting time for the vessel, and transferring technicians from the turbine.

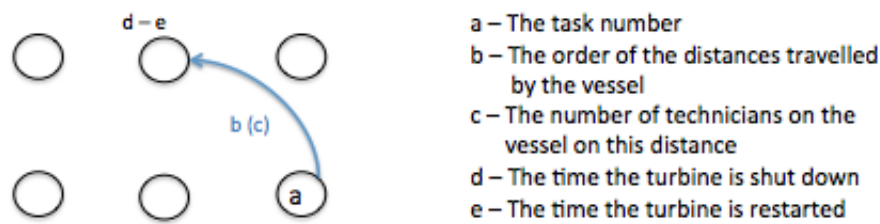


Figure S1. Explanation of the illustration figures of the numerical example of the mathematical model.

During the first shift, illustrated by Figure S2, the AV travels to wind farm 1 and the SES travels to wind farm 2. Tasks are performed in parallel by both vessels, and during the first shift, all corrective tasks are completed and both preventive tasks are started. For the second shift, illustrated by Figure S3, only the two preventive tasks are performed as these tasks are the only tasks that were not completed during the first shift. For both shifts, the entire shifts are utilized by both vessels. This complies with the weather windows being entirely open.

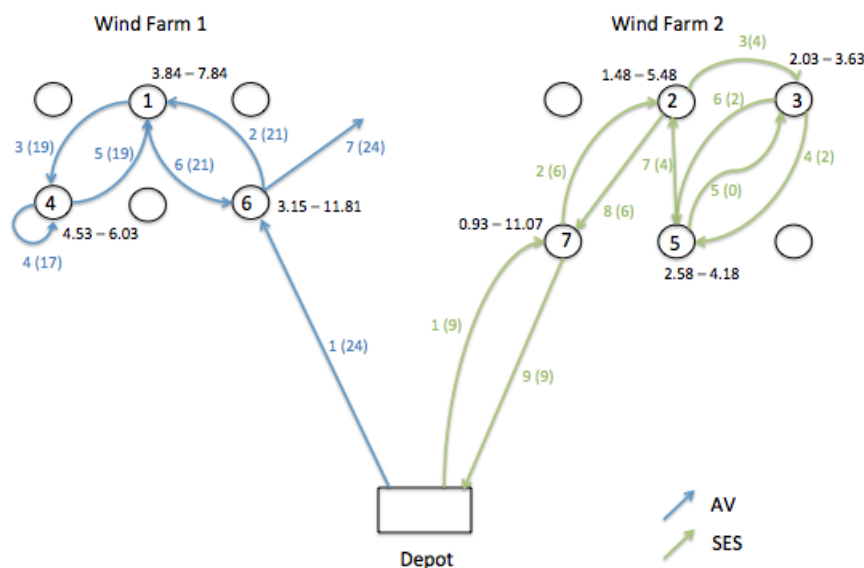


Figure S2. Illustration of shift 1 of the numerical example of the mathematical model.

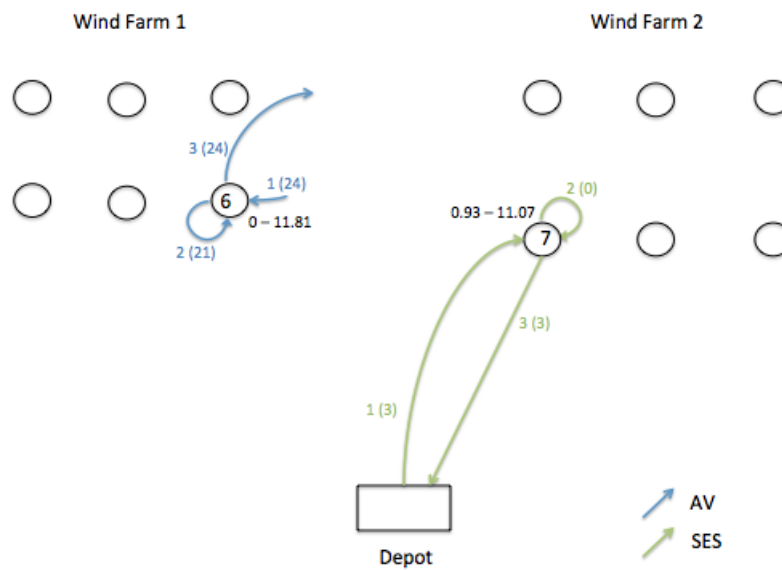


Figure S3. Illustration of shift 2 of the numerical example of the mathematical model.

When looking closely at the arrival times of the figures, it can be seen that the transportation time constraints for both internal transportation and transportation between the depot and the wind farms are complied. For example, the first task performed by the AV, task 6, is not started until the AV has arrived at the wind farm ($0\text{ h} + 3.15\text{ h} = 3.15\text{ h}$). The next task, task 1, is not started until the AV has transferred technicians to the turbine of task 6 and travelled from this turbine to the turbine of task 1 ($3.15\text{ h} + 0.5\text{ h} + 0.19\text{ h} = 3.84\text{ h}$). It can also be seen from task 6 and task 7 that the vessels finish performing tasks in time to travel to the depot or out of the wind farm within the shift (SES: $12\text{ h} - 0.93\text{ h} = 11.07\text{ h}$ and AV: $12\text{ h} - 0.19\text{ h} = 11.81\text{ h}$).

When studying the time periods the turbines are shut down, it can be seen that the tasks that are completed are shut down for the task duration plus the transfer time of the technicians. For example for task 2, the SES arrives at the turbine at 1.48 h. The technicians are then transferred to the turbine, the task is completed and the technicians transferred from the turbine ($1.48\text{ h} + 0.5\text{ h} + 3\text{ h} + 0.5\text{ h} = 5.48\text{ h}$). The figures also show that the number of technicians onboard the vessels after a turbine is visited corresponds to the technician demand of the task for both delivery and pick-up tasks. For task 3, the demand is two technicians. When task 3 is visited for delivery, the technicians at the SES decreases by two, while when task 3 is visited for pick-up, the technicians at the SES increases by two.

2. Details of the Rolling Horizon Heuristics

The main paper describes two different versions of a rolling horizon heuristic, RHH-1 and RHH-2, which differ in which decisions are fixed in the detailed time block (DTB). The mathematical formulation of the fixing strategy for RHH-1 is given by the following equations. The notation with *, e.g., x_{mvs}^* , is used for the solutions of the mathematical model solved in the iteration, and without the *, e.g., x_{mvs} , for the variables that are fixed to the solutions of the iteration.

$$\begin{aligned}
 x_{mvs}^* = 1 & \Rightarrow \sum_{u \in V_m} x_{mus} \geq x_{mvs}^* \\
 y_{ijvs}^* = 1 & \Rightarrow \sum_{u \in V_m} y_{ijus} \geq y_{ijvs}^* \\
 x_{mvs}^* \text{ and } x_{nvs}^* = 1 & \Rightarrow \sum_{u \in V_m \cap V_n} z_{mnus} \leq z_{mnvs}^* \\
 f_{ms}^* = 1 & \Rightarrow f_{ms} = f_{ms}^*
 \end{aligned}$$

The mathematical formulation of the fixing strategy for RHH-2 is given by the following equations.

$$\begin{aligned}
 x_{mvs}^* = 1 & \Rightarrow x_{mvs} = x_{mvs}^* \\
 y_{ijvs}^* = 1 & \Rightarrow y_{ijvs} = y_{ijvs}^* \\
 x_{mvs}^* \text{ and } x_{nvs}^* = 1 & \Rightarrow z_{mnvs} = z_{mnvs}^* \\
 f_{ms}^* = 1 & \Rightarrow f_{ms} = f_{ms}^*
 \end{aligned}$$

3. Details of Symmetry Breaking Constraints

The formulation of the symmetry breaking constraints added to the mathematical model presented in the main paper is given by the following equations.

$$\begin{aligned}
 \sum_{v \in V_m} \sum_{h=1}^s x_{mvsh} \geq \sum_{v \in V_n} x_{nvs}, & \quad i \in N^W, k \in K, m, n \in M_{ik}^-, \\
 & \quad s \in S \mid m < n, R_{ms} = 1, \\
 & \quad R_{ns} = 1, & (65)
 \end{aligned}$$

$$\begin{aligned}
 \sum_{h=1}^s f_{mh} \geq f_{ns}, & \quad i \in N^W, k \in K, m, n \in M_{ik}^-, s \in S \\
 & \quad \mid m < n, R_{ms} = 1, R_{ns} = 1, & (66)
 \end{aligned}$$

$$\begin{aligned}
 x_{nvs} \leq \sum_{u=1}^v x_{mus} + f_{ms}, & \quad i \in N^W, k \in K, m, n \in M_{ik}^-, \\
 & \quad v \in V_m, s \in S \mid m < n, \\
 & \quad R_{ms} = 1, R_{ns} = 1, & (67)
 \end{aligned}$$

$$\begin{aligned}
 x_{nvs} \leq \sum_{u=1}^v x_{mus} + f_{(m-|M^-|)_s}, & \quad i \in N^W, k \in K, m, n \in M_{ik}^+, \\
 & \quad v \in V_m, s \in S \mid m < n, \\
 & \quad R_{ms} = 1, R_{ns} = 1. & (68)
 \end{aligned}$$

Constraints (65)–(68) concern the order of the tasks performed across shifts. Tasks cannot be performed during a shift unless all tasks of the same task type within the same wind farm of lower indices are performed during the same or earlier shifts. This is ensured by Constraint (65). The same applies for completing tasks which is ensured by Constraint (66). Constraints (67) and (68) handle the chosen symmetry restrictions of vessels. If multiple vessels are located within the same wind farm, then the vessels of lower indices must perform the tasks of lower indices for tasks of the same type. Constraints (65)–(68) only apply for tasks where all necessary spare parts and equipment are available from shift $s = 1$. This is to avoid that tasks of lower indices that cannot be performed until later shifts restrict tasks of higher indices to be performed in earlier shifts.

$$\begin{aligned}
 t_{mvs} \leq t_{nvs} + (1 - x_{nvs})T_s^{SHIFT}, & \quad i \in N^W, k \in K, m, n \in M_{ik}^-, \\
 & \quad v \in V_m, s \in S \mid m < n, \\
 & \quad R_{ms} = 1, R_{ns} = 1,
 \end{aligned} \tag{69}$$

$$\begin{aligned}
 t_{mvs} \leq t_{nvs} + (1 - x_{nvs})T_s^{SHIFT}, & \quad i \in N^W, k \in K, m, n \in M_{ik}^+, \\
 & \quad v \in V_m, s \in S \mid m < n, \\
 & \quad R_{ms} = 1, R_{ns} = 1.
 \end{aligned} \tag{70}$$

Constraints (69) and (70) concern the order of the tasks performed within a shift. If task m and task n are performed during shift s , are of the same task type, are located in the same wind farm, and if task m is of lower index than task n , then the constraints ensure that task m has a lower start time than task n . Constraint (69) applies for delivery tasks, and Constraint (70) for pick-up tasks. As for Constraints (65)–(68), Constraints (69) and (70) only apply for tasks where all necessary spare parts and equipment are available from shift $s = 1$.

$$\begin{aligned}
 z_{mnvs} = 0, & \quad i \in N^W, k \in K, m, n \in M_{ik}^-, \\
 & \quad v \in V_m, s \in S \mid m > n, \\
 & \quad R_{ms} = 1, R_{ns} = 1,
 \end{aligned} \tag{71}$$

$$\begin{aligned}
 z_{mnvs} = 0, & \quad i \in N^W, k \in K, m, n \in M_{ik}^+, \\
 & \quad v \in V_m, s \in S \mid m > n, \\
 & \quad R_{ms} = 1, R_{ns} = 1,
 \end{aligned} \tag{72}$$

$$\begin{aligned}
 z_{nmvs} = 0, & \quad i \in N^W, k \in K, m \in M_{ik}^-, n \in M_{ik}^+, \\
 & \quad v \in V_m, s \in S \mid m < n - |M^-|, \\
 & \quad R_{ms} = 1, R_{ns} = 1,
 \end{aligned} \tag{73}$$

$$\begin{aligned}
 z_{mnvs} = 0, & \quad i \in N^W, k \in K, m, n, l \in M_{ik}^-, \\
 & \quad v \in V_m, s \in S \mid m < l < n, \\
 & \quad R_{ms} = 1, R_{ns} = 1,
 \end{aligned} \tag{74}$$

$$\begin{aligned}
 z_{mnvs} = 0, & \quad i \in N^W, k \in K, m, n, l \in M_{ik}^+, \\
 & \quad v \in V_m, s \in S \mid m < l < n, \\
 & \quad R_{ms} = 1, R_{ns} = 1.
 \end{aligned} \tag{75}$$

The z_{mnvs} variables of tasks of the same type within the same wind farm are handled by Constraints (71)–(75). Constraints (71) and (72) restrict that a task m of a higher index than task n are performed directly before task m for delivery and pick-up tasks, respectively. Constraint (73) ensures that a pick-up task n cannot be performed directly before a delivery task m if the delivery task corresponding to task n is of a higher index than task m . If there exists a task l that is of higher index than task m and of lower index than task n , and if task m, l and n are of the same task types and located in the same wind farm, then task m cannot be performed directly before task n . This is restricted by Constraints (74) and (75) for delivery tasks and pick-up tasks, respectively. Constraints (71)–(75) only apply for tasks where all necessary spare parts and equipment are available from shift $s = 1$.

4. Data Used to Generate Test Instances

This section outlines the input data that is used to generate scenarios to test in the simulations. In order to generate realistic scenarios, best practice for the offshore wind industry has been applied where possible. Various sources and expert opinions have been used to find different parameter data.

Energy from offshore wind is a relatively new industry and access to input data is limited. Reasonable estimates has therefore been used when there is no data available. The input data that is used when generating scenarios is mainly based on a reference case created for verification of O&M simulation models for offshore wind farms by Dinwoodie et al. in [1] and on conversations with Bjørn Ivar Vold, asset management engineer in Wind Offshore in Statkraft.

Three types of vessels are included in the vessel fleet of the scenarios generated, AVs, regular CTVs and SESes. Speed, transportation costs, maximum offshore time, and wave height limits of the three vessel types are given in Table S4. The speed and wave height limits for regular CTVs and the speed of AVs are found in the reference case by Dinwoodie et al. in [1]. Wave height limits for AVs are based on the results of a computational study on wave limits from [2], while wave height limits for SESes are, together with the speed of SESes, taken from the vessel specifications of the SES Umoe Mandal WaveCraft [3]. Transportation costs for regular CTVs are given in [4]. As data for AVs and SESes are limited, costs of these vessels are chosen within a reasonable estimate compared to the costs of regular CTVs. Daily cost rates are given in [5].

Table S4. Vessel fleet input data used to generate scenarios.

	AV	SES	Regular CTV
Speed of vessel (knots)	12	45	20
Transportation costs (EUR/h)	1125	383	225
Maximum offshore time	4 weeks	1 shift	1 shift
Wave height limits (m)	3.0	2.5	1.5
Daily cost rates (EUR/day)	6950	16,700	2360

Input data on different types of maintenance tasks are given in Table S5. Except for triggered alarms, these categories and the corresponding data are taken from the reference case by Dinwoodie et al. in [1]. The categories are based on types of maintenance tasks and their respective failure rates defined in the Reliawind project, a project that identified and analyzed critical failures of wind farms [6]. Data on triggered alarms are based on conversations with Bjørn Ivar Vold. It is assumed that a corrective task can only happen after an alarm is triggered, however not all triggered alarms result in maintenance tasks, some can be false alarms. The failure rate of a triggered alarm is therefore set to be equal to the total failure rate of a corrective task happening at the turbine and the rate of false alarms. The rate of false alarms is assumed to be approximately 10 % of the total triggered alarms.

Only tasks that can be performed by AVs, regular CTVs or SESes have been included in the data set, tasks that require jack-up barges, such as major replacements, are omitted. Task durations, yearly failure rates, what vessel types that can perform the tasks and what tasks that require the vessel to stay at the turbine when performed are given in Table S5.

Table S5. Maintenance task input data used to generate scenarios.

	Triggered Alarms	Manual Reset	Minor Repair	Medium Repair	Major Repair	Preventive Maintenance
Task duration (h)	0.5	3	7.5	22	26	60
Required technicians	2	2	2	3	4	3
Yearly failure rate	12	7.5	3.0	0.275	0.04	1
Vessel type	All	All	All	All	AV	All
Requires vessel to stay at turbine	No	No	No	No	Yes	No

The number of desired preventive tasks, β , is set to 70% of the demand in the planning period. Of the total number of yearly preventive tasks, 50% are allocated to be performed during summer, 25% during spring and 25% during fall. The power output level of when it is considered as more attractive to produce power than to perform additional preventive maintenance, α , is set to 25% of the maximum power output. This corresponds to a wind speed just below 10 m/s. Incentive to perform extra preventive tasks is then given when the wind speed is outside the range where a turbine produce more than 25% of maximum output, i.e., when the wind speeds are below 10 m/s or above the cut off speed.

Weather forecasts for the scenarios generated are based on weather data collected from 2004–2012 at the offshore research platform FINO 1. This is the same weather data as used for the reference wind farm in [1]. FINO 1 is situated in the North Sea, approximately 45 km to the north of Borkum, Germany, and can be considered representative of Central North Sea conditions [7]. The price of energy is set to 90 EUR/MWh, including both the electricity selling price and subsidies.

For comparison purposes when analyzing the mathematical model, a reference case of two wind farms has been constructed to form a basis for the scenarios generated. Data such as capacity of turbines, length of shifts and vessel fleet are fixed for this reference case and apply to all scenarios tested if not otherwise stated. The time unit used in the scenarios generated is hours, and, hence, there are 24 time units in one day. The fixed input data are summarized in Tables S6 and S7.

Table S6. General input data used to generate scenarios.

Number of wind farms	2
Distance between wind farms (km)	50
Number of AVs	1
Number of SESes	1
Number of regular CTVs	0
Length of shifts (h)	12
Time to transfer technicians from vessel to turbine (h)	0.5
Season	Summer

Table S7. Wind farm specific input data used to generate scenarios.

	Wind Farm 1	Wind Farm 2
Capacity of turbines (MW)	5	3.6
Distance from depot (km)	80	70
Distance between turbines (km)	1	1

5. Detailed Results from the Computational Study

5.1. Optimality Gaps for Full Model After Two Hours

For all tested problems with a planning period of one shift at least one solution is found when solving the full model. However not all problems are solved to optimality. Figure S4 presents the 95% confidence intervals of the gaps in the solutions of these problem combinations. The exact model can solve realistic problems, both for current and future offshore wind farms sizes, within a reasonable gap in objective function value for a planning period of one shift. The exact model struggles to solve larger problems for longer planning periods than one shift. For several of these problems tested, no solution is found within the memory capacity of the computer.

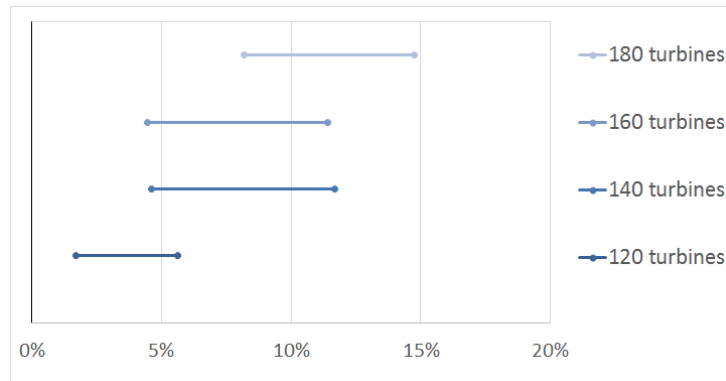


Figure S4. 95% confidence interval for the gap of the solutions when solving the exact model for a planning period of one shift and different numbers of turbines.

5.2. Comparing RHH-1, RHH-2, and the Full Model

A full comparison between the full model, RHH-1, and RHH-2 is conducted on the instances with three shifts. The results of testing RHH-1 are presented in Table S8. Both RHH-1 and RHH-2 are able to find feasible solutions to larger instances than the full model, and the heuristics finds solution of equal or higher quality than the exact model for many of the problems tested.

Table S8. Results for RHH-1 on instances with three shifts. RHH-2 found feasible solutions to all but 3 of the same instances.

Shifts, Turbines	Feasible	Better or Equal to Exact
3, 120	18	14
3, 140	16	11
3, 160	13	9

Figures S5–S7 present 95% confidence intervals for the difference in the performance of the three methods. In the figures, ST refers to solution time and OV refers to objective function value. Figures S5 and S6 show how RHH-1 and RHH-2 perform better than the exact model in terms of solution time. For RHH-2 the difference in objective function value is relatively small, while for the RHH-1, the objective function values are generally higher than for the exact model.

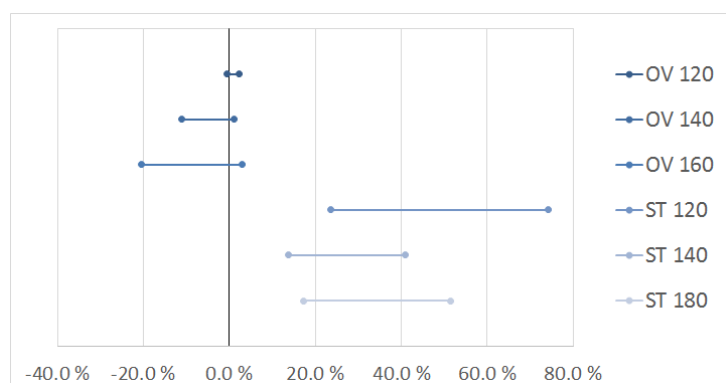


Figure S5. 95% confidence interval for the difference in objective function value and solution time for the exact model and RHH-1 for problems of 120, 140 and 160 turbines, with a planning period of three shifts. Positive differences mean that the values of the exact model are greater than for RHH-1.

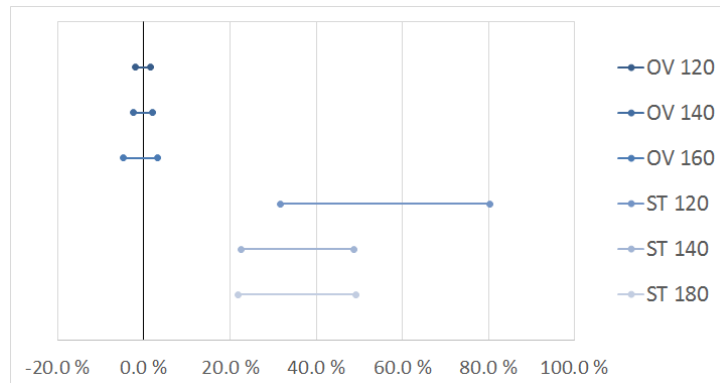


Figure S6. 95% confidence interval for the difference in objective function value and solution time for the exact model and RHH-2 for problems of 120, 140 and 160 turbines, with a planning period of three shifts. Positive differences mean that the values of the exact model are greater than for RHH-2.

From Figure S7 it can be seen that the solutions of RHH-1 are in general more expensive than the solutions of RHH-2 for the problems tested. In addition, the confidence interval for the difference in RHH-1 and the exact model is much larger than for RHH-2 and the exact model. This means that RHH-2 provides solutions of less variable quality than RHH-1 and that the performance of RHH-2 is more stable than the performance of RHH-1.

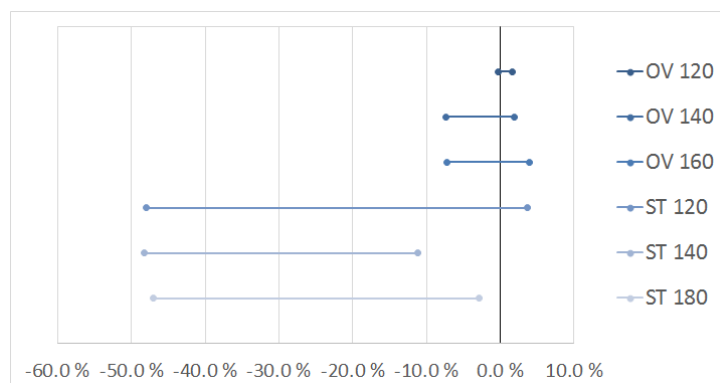


Figure S7. 95% confidence interval for the difference in objective function value and solution time for RHH-2 and RHH-1 for problems of 120, 140 and 160 turbines, with a planning period of three shifts. Positive differences mean that the values of RHH-2 are greater than for RHH-1.

Based on the results of testing the three models, RHH-2 is considered as the best performing model for planning periods of more than one shift. RHH-2 finds at least one solution to more problems than both the exact model and RHH-1, it provides solutions of high and stable quality and it has the lowest solution time for the problems tested. As RHH-2 performs better than RHH-1, this implies that that for this problem, fixing more decisions in the DTB is more efficient than keeping several variables free during later iterations. It seems that too much time is spent on re-assessing these variables, and that this prevents that solutions of higher qualities are found. RHH-1 is therefore discarded in favor of RHH-2 and not further tested.

RHH-2 was tested without the symmetry breaking constraints for the twenty problems of the problem combinations with a planning period of three shifts and 120 and 140 turbines. From Table S9 and Figure S8, it seems that RHH-2 without the symmetry breaking constraints performs equal to or better than with the symmetry breaking constraints in terms of objective function value. This implies that the added symmetry breaking constraints eliminate solutions of high quality. However, as the table shows, without the symmetry breaking constraints RHH-2 are not able to solve all the problems tested. In addition, the solution time increase significantly for several of the problems. As the solution

quality is not reduced considerably, it is considered as more important to find good solutions to more problems, than better solutions to fewer problems.

Table S9. Comparison of the solutions of RHH-2 with symmetry breaking constraints (SBC) and without SBC. The table includes the number of problems where at least one solution is found, the number of problems where RHH-2 with SBC found better solutions than without SBC (with SBC > without SBC), equal solutions (with SBC = without SBC), and worse solution (with SBC < without SBC).

	No. of Problems Where at Least One Solution Is Found without SBC	With SBC > Without SBC	With SBC = without SBC	With SBC < Without SBC
2 shifts - 120 turbines	19	7	5	8
2 shifts - 140 turbines	18	16	0	4

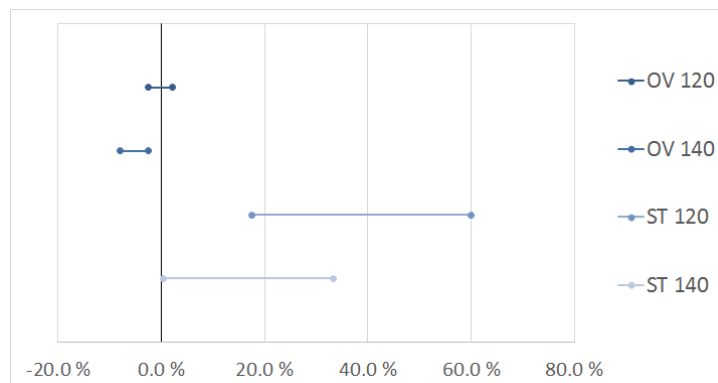


Figure S8. 95% confidence interval for the difference in objective function value and solution time for RHH-2 without and with symmetry breaking constraints. Positive differences mean that the values of RHH-2 without the symmetry breaking constraints are greater than with the symmetry breaking constraints.

References

1. Dinwoodie, I.A.; Endrerud, O.E.V.; Hofmann, M.; Martin, R.; Sperstad, I.B. Reference Cases for Verification of Operation and Maintenance Simulation Models for Offshore Wind Farms. *Wind Eng.* **2015**, *39*, 1–14.
2. Sperstad, I.B.; Halvorsen-Weare, E.E.; Hofmann, M.; Nonås, L.M.; Stålhane, M.; Wu, M. A Comparison of Single- and Multi-parameter Wave Criteria for Accessing Wind Turbines in Strategic Maintenance and Logistics Models for Offshore Wind Farms. *Energy Proced.* **2014**, *53*, 221 – 230.
3. The Maritime Journal. Design for Surface Effect Ship (SES) WFSV. Available online: <http://www.maritimejournal.com/news101/marine-renewable-energy/design-for-surface-effect-ship-ses-wfsv> (accessed on 21 February 2015).
4. Dai, L.; Stålhane, M.; Utne, I. Routing and Scheduling of Maintenance Fleet for Offshore Wind Farms. *Wind Eng.* **2015**, *39*, 15–30.
5. Tavner, P. *Offshore Wind Turbines: Reliability, Availability and Maintenance*; The Institution of Engineering and Technology: Stevenage, UK, 2012.
6. Wilkinson, M.; Harman, K.; Hendriks, B.; Spinato, F.; van Delft, T.; Garrad, G.L.; Thomas, U.K. Measuring wind turbine reliability, results of the reliawind project. In Proceedings of the EWEA Conference, Amsterdam, The Netherlands, 29 November–12 December 2011; pp. 1–8.
7. Forschungsplattformen in Nord- und Ostsee. Fino 1. Location. Available online: <http://www.fino1.de/en/location-sea-floor-waves-wind> (accessed on 15 March 2015).